Targeted PD-L1 PLGA/liposomes-mediated luteolin therapy for effective liver cancer cell treatment

Xinqiao Cao and Bing Wang [ORCID]

Abstract

Stealth PLGA/Liposome nanoparticles (NPs) modified with tumor-targeting PD-L1 antibody for systemic delivery of luteolin for liver cancer were prepared. The morphologies and therapeutic effects of luteolin-loaded PD-L1 targeted stealth PLGA/Liposomes (L-PD-SP/Ls) *in vitro* were analyzed. Functional L-PD-P/L NPs composed of PLGA, DOPC and DSPE-PEG display low cell cytoxicity in HepG2 cells, and has more cell uptake ability than P/Ls NPs. L-PD-SP/Ls was more effective in inhibiting HepG2 cell proliferation than free luteolin in solution ($p < 0.05$) and luteolin-loaded P/Ls ($p < 0.05$). Compared with the cell control group and the non-PD-L1 targeted group, the mediated effect of PD-L1 can significantly enhance the uptake of drugs by cells, and L-PD-SP/Ls can significantly reduce the expression of Bcl-2 and increase the level of LDH in cells. Our findings collectively support the utility of PD-L1-targeted P/L NPs as a potentially effective drug delivery system.

Keywords

Stealth liposomes, liver cancer, PD-L1, targeting, drug therapy

Introduction

Currently, the most commonly used anti-tumor drugs are bioalkylating agents, antimetabolite and oxidation-reduction cycling agents, etc., including over 10 drugs such as cyclophosphamide, bleomycin, cisplatin and leukeran.[1] Hepatocellular carcinoma (HCC) is an aggressive primary liver cancer that causes serious harm to human health, with a high rate of recurrence and metastasis. Chemotherapy,[2] which can improve the therapeutic effects and improve the survival of patients, represents the main means of clinical treatment. Although new chemotherapeutic drugs are being approved and applied, drug resistance[3] of malignancies is still the leading cause of chemotherapy failure of tumors. In addition, the current clinical anti-cancer drugs have caused a lot of adverse effects to human bodies, such as thrombocytopenia and diminished immunity.[4,5] Traditional Chinese medicines demonstrate significant effects in the comprehensive treatment of tumors. Luteolin is a natural flavonoid compound that exists mostly in the form of glycosides in a variety of plants, and is clinically used for cough, expectorant, anti-inflammation, cardiovascular disease, inflammatory demyelinating disease, and dry skin itching, etc.[6,7]

Recent studies also found that luteolin has strong anti-viral activity against coxsackie virus, rotavirus, adeno-virus and other viruses.

In recent years, studies on anti-tumor effects of luteolin focus on its inhibition of tumor proliferation and promotion of apoptosis. Programmed death ligand-1 (PD-L1), which is highly expressed on the surface of HCC cells, also associated with poor prognosis of liver cancer. The PD-L1 targeting nano-drug delivery system display[8,9] the double advantages of active targeting of the PD-1 and passive targeting of the nanometer delivery system, and it can achieve the targeted delivery of drugs to tumor tissues, thereby improving the efficacy of drugs effectively and reducing side effects.

Lactate dehydrogenase (LDH) is a protein within the human body as well as a metabolic enzyme that produces

Department Of Radiotherapy, Heng Shui City People's Hospital, Hengshui, China

Corresponding author:
Bing Wang, Heng Shui City People's Hospital, No. 180, East Renmin Road, Hengshui 053000, China.
Email: wangbing19007506@126.com

lactic acid.[10–12] Studies have shown that LDH always maintains a low expression level within the body in the normal population, while it is highly expressed in a variety of tumors. Gypsophila elegans isoorientin and many other traditional Chinese medicines can effectively inhibit the survival of HepG2 cells and increase the release of LDH. Therefore, the anti-tumor activity of luteolin is also studied from the perspective of LDH. It produces a large amount of lactic acid as the metabolite when accumulating in the body. Of coure, contributions of increases in acidity in the tumor microenvironment (for poly lactic acid/LDH assay-mediated increase in lactate) may cause an elevation in metastasis, angiogenesis and more importantly, immunosuppression.[13,14] Herein, we aimed to investigate the possible mechanisms underlying the impact of luteolin on the proliferation and migration of human liver cancer cells, and we constructed PD-L1-modified stealth PLGA/Liposomes[15,16] to load luteolin to enhance the effects of drugs on cells, thus confirming the effectiveness of the constructed targeted nano-delivery system and providing experimental basis for other related studies.

Materials and methods

Experimental materials

Poly (D,L-lactic-co-glycolic acid) ($M_w = 10,000$ lactic/glycolic acid ratio = 60/40) was purchased from Shandong Key Laboratory of Medical Polymer Material (China). DSPE-PEG2000-NH$_2$ (1,2-distearoyl-sn-glycero-3-phosphoethanolamine-N- [amino (polyethylene glycol)-2000]), Cholesterol (Chol) and DOPC were purchased from Avanti Polar Lipids (USA). The human liver cancer cell line HepG2 was purchased from ATCC, and conventional resuscitation and subculture were performed. Luteolin, MTT and DMSO were purchased from sigma. The reagents for total RNA extraction and real-time fluorescent quantitative analysis from TakaRa (Japan). The mouse anti-human alpha-tubulin antibody, the mouse anti-human LDHA antibody, the horseradish peroxidase-labeled goat anti-mouse and the goat anti-human secondary antibody were purchased from Bioworld (USA). Primers and sequencing were performed by Shanghai Jukang Biotechnology Co., LTD.

Preparation of luteolin-loaded PD-L1 targeted stealth PLGA/liposomes (L-PD-SP/Ls)

Luteolin-loaded PLGA NPs were prepared using a modified solvent extraction/evaporation double emulsion method according to the Onyango.[14] In brief, 5.0 mg luteolin and 5.0 mg PVA were dissolved in 1.0 mL deionized water as the internal aqueous phase.

The organic phase was prepared by dissolving 25.0 mg PLGA in 5.0 ml dichloromethane solution. The internal aqueous solution was added into the organic phase under sonication for 10 s at an output of 50 W. The external aqueous of 7.0 mL PBS (0.1 mol/L) solution was added into the above emulsion with sonication for 60 s at an output of 80 W. The double emulsion was evaporated with a vacuum rotary evaporator (RE52CS, Beijing Liuyi Biotechnology Co., LTD) to allow the organic solvent to completely evaporate.

PLGA/liposomes were prepared using the thin-film hydration method. Briefly, DOPC, cholesterol and DSPE-PEG2000-NH$_2$ (weight ratio of 5: 4: 1, 20.0 mg total lipids) were dissolved in 4.0 ml chloroform at room temperature to obtain the organic phase. Chloroform was evaporated to form lipid thin film. The above 1.0 mL PLGA NPs solution was added into the flask with liposome thin film, and then the solution was sonicated with sufficient hydration (3 mins, 100 W). After 10 mins at room temperature, liposomes were mixed with 200 μL DSPE-PEG-NH$_2$ (10.0 mg/mL) and incubated at 37 °C for a further 10 mins. For PD-L1 conjugation, the PD-L1 was dissolved in alkaline solution (pH = 10) with EDC (1.0 mg/mL), incubated with PLGA/liposome NPs for 24 hours at room temperature. After that, low molecular weight impurities were dialyzed against 0.1 mol/l PBS for 6 hours with a dialysis bag ($M_w = 1000$).

Average particle size and size distribution were determined via Zetasizer 3000HS laser particle size analyzer (Malvern Instruments Limited, United Kingdom) at 25 °C. The detection angle for the size measurements in the zetasizer is 173°. The original solution (3.0 mg/ml) was diluted 5 times by PBS (0.1 mol/l) to the final 3.0 ml.

The drug encapsulation efficiency (DEE) and the drug loading capacity (DLC) was determined by dialysis method. The final prepared luteolin-loaded microspheres were placed in dialysis bags (Mw = 12,000) for 3 hours. The volume of PBS (0.1 mol/l) dialysis fluid was 500 ml. After dialysis, the drug concentration in the solution outside the dialysis bag was measured. The concentration of luteolin was determined by UV/Vis spectroscopy (Beijing Purkinje general instrument Co., Ltd. China) at 328 nm.

Characterization of PD-SP/Ls and L-PD-SP/Ls
Detection of cell proliferation
Inhibitory effects of different loaded luteolin on liver cancer cells. The 96-well cell plate was used, with the cell concentration adjusted to 5×10^4/ml. The cells were cultured for 24 hours overnight, and then in luteolin-containing medium for 48 hours. An increasing amount of different loaded luteolin (PBS control, free

luteolin, L-SP/Ls and L-PD-SP/Ls) were added and incubated (from 0 to 100 µg/ml) for 24 h at 37 °C, respectively. Different incubation times of 6 hours, 12 hours, 24 hours and 48 hours were also selected to detect the cell inhibition rate when the solution concentration was 20 µg/ml. Each well was added with 10 ul of MTT solution, and the plate was cultured in an incubator at 37 °C in a humidified atmosphere of air and 5% CO_2 for 4 hours, with the supernatant discarded. 100 ul of DMSO was added, and then the cells were shaken for 10 mins and placed in the microplate reader for measurement of absorbance (OD) at a wavelength of 490 nm, with 630 nm as the reference wavelength. The experiments were repeated in triplicated and the average values were used.

Inhibitory effects of drug-loading nanoparticles on liver cancer cells. A total of 4 groups were set in the experiment, namely the liver cell group (blank control group), the free luteolin group, the luteolin-loading liposome group (L-SP/Ls) and the L-PD-SP/Ls group. The 96-well cell plate was used, with the cell concentration adjusted to 5×10^4/ml. The cells were cultured for 24 hours overnight, and then in luteolin-containing medium for 48 hours. Each well was added with 10 ul of MTT solution, and the plate was cultured in an incubator at 37 °C in a humidified atmosphere of air and 5% CO_2 for 4 hours, with the supernatant discarded. 100ul of DMSO was added, and then the cells were shaken for 10 mins and placed in the microplate reader for measurement of absorbance (OD) at a wavelength of 490 nm, with 630 nm as the reference wavelength. The experiments were repeated in triplicated and the average values were used.

Cell uptake detection. A total of 5×10^5 HepG2 cells in the logarithmic growth phase were harvested and seeded in a 6-well plate with cell climbing pieces.[13] After the 24 hours incubation, the prepared fluorescein isothiocyanate-labeled SP/Ls (SP/Ls-FITC) and FITC labeled PD-SP/Ls (PD-SP/Ls-FITC) were added, and the 6-well plate was placed in an incubator for further culture. At specific time points, the cells climbing pieces were taken out with camps, washed with cold PBS buffer solution for 3 times and placed in 4% paraformaldehyde for fixation. And then the climbing pieces were taken out, placed upside down on the slide, and mounted with 50% glycerol. Laser confocal microscopy (Media Cybernetics, Washington, USA) was performed to observe the slide under excitation light at a wavelength of 488 nm.

Detection of cell migration. Cells were seeded in 24-well plates at the concentration of 5×10^5 per cells. After the cells had formed nearly a single layer, straight lines in the 24 wells were evenly drawn with a 10 µl tip. The cells were washed for three times with PBS, added with 1% fetal bovine serum, and continued to be incubated for 48 hours. Scratch width was measured at 0 hours and 48 hours, respectively, with the average migration distance expressed as (scratch width at 0–48 hours)/2.

Detection of expression of Bcl-2 and LDH mRNA[17,18]. Trizol was added at 48 hours after the cells were treated with drug-loading liposomes for lysis, and total RNA extraction was performed using RNase-free at a low temperature. The expression of Bcl-2 and LDHA mRNA was detected using real-time fluorescence quantitative analysis. The upstream primer sequence of the designed LDHA was 5′-CCAACATGGCAGCCTTTTCC-3′, the downstream primer sequence was 5′-TCACGTTACGC TGGACCAAA-3′, and the amplified fragment was 149 bp in length. The upstream primer sequence of the designed Bcl-2 was 5′-TTCTTTGAGTTCGGTGGG GTC-3′ and the downstream primer sequence was 5′-TGCATATTTGTTTGGGGCAGG-3′. The reaction conditions were as follows: pre-denaturation at 94 °C for 2 mins in 28 cycles, denaturation at 94 °C for 30 s, annealing at 60 °C for 30 s, and 72 °C for 30 s. After the completion of the cycle, the primers were extended at 72 °C for 5 mins. Analysis of LDH mRNA expressions was performed.

Detection of expression of LDH protein. The protein was extracted from cell culture supernatant at 72 hours after the prepared drug-loading liposome was added, and subsequently subjected to 10% SDS-PAGE, membrane transfer, mounting and membrane washing.[19] The protein was incubated with primary antibody at 4 °C overnight, and antibody against LDHA was diluted at 1: 1000. The antibody against the internal reference α-tubulin was diluted at 1: 10000, and the secondary antibody was diluted at 1: 10000. Chemical fluorescence visualization was performed at 1 hour after incubation at room temperature, and expression of LDH protein was analyzed. Similarly, the sample was treated according to the LDH kit instructions, and the A value of the sample was measured at 450 nm with microplate microscope, and the LDH activity was calculated.

Statistical methods

The data were recorded and processed by the SPSS 19.0 software package. The data measurement data were expressed by mean ± standard deviation. The single-factor ANOVA analysis was used for comparison of the results, and the LSD-t method for pairwise comparison. Comparison between the two groups was performed using the independent-sample *t* test and

$p < 0.05$ indicated that the difference was statistically significant.

Results and discussion

Formulation of L-PD-SP/Ls

PLGA/lipid complexes have many advantages as delivery vehicles. They combine the properties of liposomes and PLGA and can be easy modified by antibody. Liposome is an artificial vesicle, with simlar cell membrane structure, which composed of one or more concentric phospholipid bilayers and used especially to deliver different drugs to body cells.[20,21] To improve the drug delivery rate and the controled release function of Luteolin, Liposome was used to encapsulate the drug loaded PLGA. A schematic illustration of the preparation L-PD-SP/Ls is presented in Figure 1(a). First, luteolin loaded PGLA microspheres were prepared, then the suspension of PLGA microspheres was used as the aqueous phase of liposome hydration, and liposomes were prepared by thin-film method. Of course, PEGylated P/Ls can be assembled by the thin-film hydration method from DSPE-PEG2000-NH$_2$, DOPC, and cholesterol. The DSPE-PEG-NH$_2$ component mean that amine groups are present on the surface of stealth P/Ls. PD-L1 antibody is connected to the surface of the microsphere by coupling agent of EDC. Of course, luteolin was first encapsulated inside the PLGA microsphere, and then, during the preparation of the liposome, it was loaded again. The second encapsulation increased the encapsulation efficiency ($92.0 \pm 1.9\%$) and the drug loading capacity ($8.6 \pm 0.6\%$). TEM showed that the drug was first encapsulated into PLGA NPs and then loaded with PLGA NPs by lipid membrane to form large microspheres (Figure 1(b)).

Physical characterization of L-PD-SP/Ls

The ultraviolet spectrum of the modified PD-L1 microspheres is shown in Figure 2(a). As can be seen from the figure, the unmodified PD-L1 antibody has an obvious absorption peak at 280 nm and is relatively strong. When the microsphere was modified by the antibody, the absorption peak at 280 nm was significantly reduced, indicating that the surface of the microsphere contained PD-L1 antibody. The unmodified microspheres had no obvious absorption peak.

The average encapsulation rate of the drug was $85.6 \pm 0.43\%$ by dialysis. The particle size distribution and dispersibility index of the samples in the aqueous solution were shown in Figure 2(b) and (c). The average particle size of L-SP/Ls and L-PD-SP/Ls were 99.1 ± 5.75 nm and 159.3 ± 7.45 nm, respectively, and their PDIs were 0.198 and 0.239, respectively. The size of PD-L1-modified nano-liposomes was increased. The particle size is basically the same as that of circular microspheres shown in TEM image (Figure 1(b)). The electric potential of the empty PD-L1 antibody L-SP/Ls was -12.5 ± 3.76 mV, as compared with that of the PD-L1-modified L-SP/Ls [(-3.2 ± 0.44) mV].
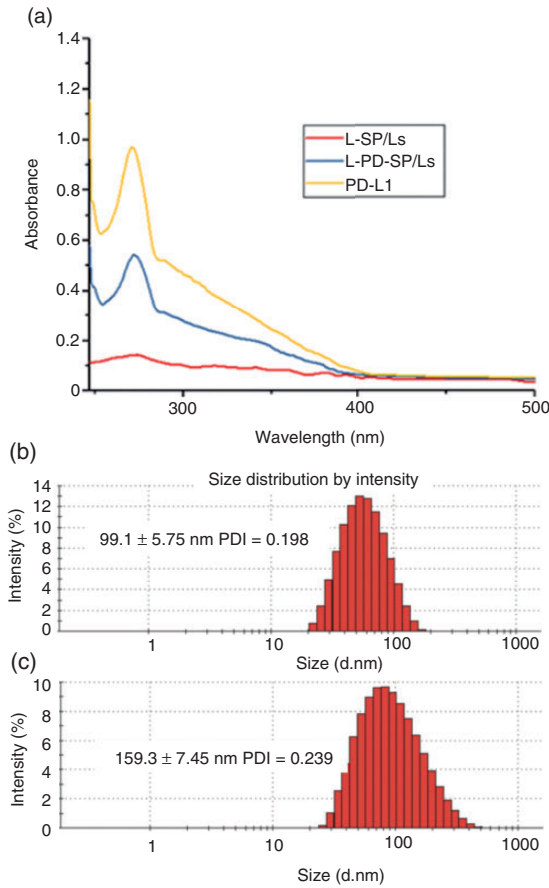
In vitro cytotoxicity of L-PD-SP/Ls

In order to evaluate the cytotoxicity of L-PD-SP/Ls compared with that of the other formulations, HepG2 cells were also treated with different formulations at different concentrations at 24 hours, and the inhibitory effect on cell growth was determined by
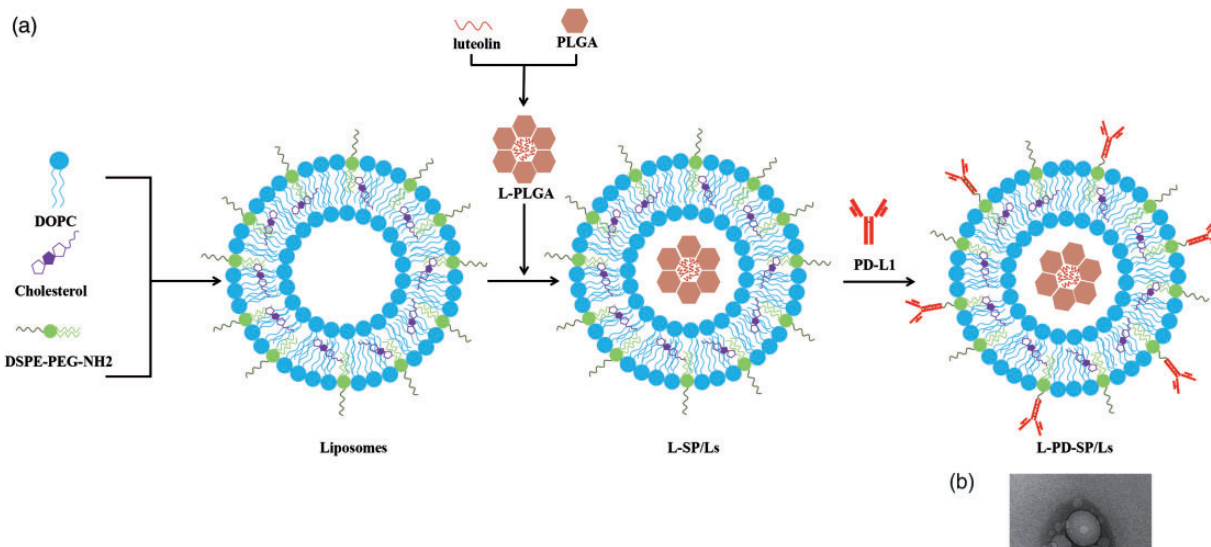

Figure 1. Schematic of the preparation of L-PD-SP/Ls (a) and TEM image of L-PD-SP/Ls (b).

MTT assays (Figure 3). It can be seen that the cytotoxicity increased as the concentration increased from 0 to 100 µg/ml. Then we selected 20 µg/ml to study the changes of cell proliferation with culture time.

Figure 2. (a) Ultraviolet spectrogram. Diagram of particle size distribution of L-SP/Ls (b) and L-PD-SP/Ls (c).
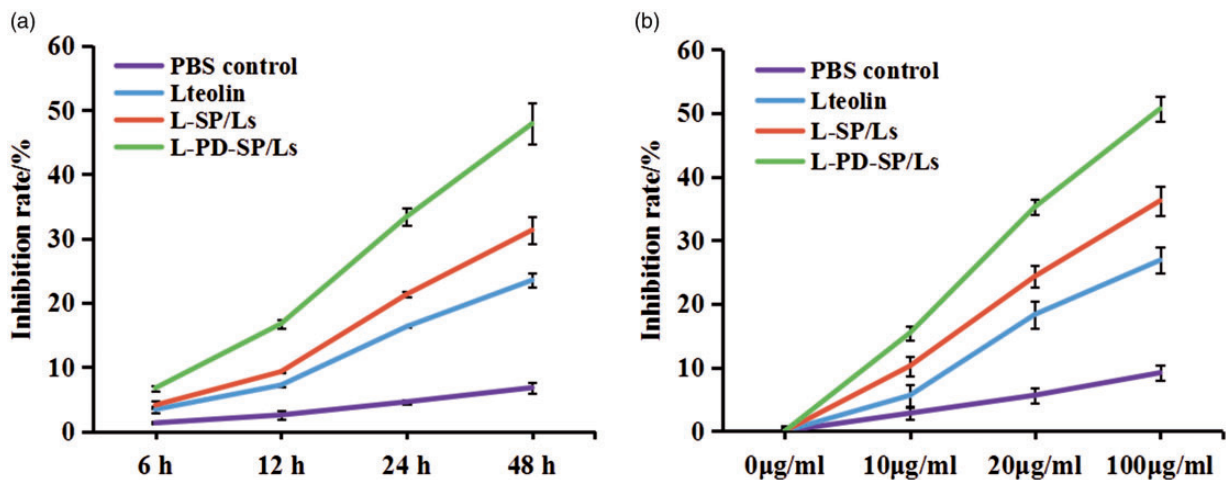
The curve of inhibition of HepG2 cells by PBS control, free luteolin, L-SP/Ls and L-PD-SP/Ls are shown in Figure 3(a), which showed that the inhibition rate were $6.82 \pm 0.87\%$, $23.54 \pm 1.1\%$, $31.33 \pm 2.1\%$ and $47.89 \pm 3.22\%$ when lutelin was administered at 20 µg/ml for 48 hours. The results showed that compared with free luteolin, the drug loaded NPs both induced the lowest cell viability. After treatment with L-SP/Ls, cell growth was inhibited by $\sim$36%. More importantly, cell growth was inhibited by 50% after treatment with L-PD-SP/Ls, which effectively delivered luteolin to the HepG2 cells by PD-L1 mediated. The results showed that the sensitivity of HepG2 cells to luteolin was greatly increased in the L-PD-SP/Ls group, while that in the L-SP/Ls was increased modestly. In summary, it can be concluded that L-PD-SP/Ls induced the highest level of inhibition and the highest levels of cytotoxicity.

Cellular uptake of PD-SP/Ls by laser confocal microscopy

Simlar with the other receptor and ligand mediated cell endocytosis path such as the folate, the PD-L1 receptor is highly expressed in liver cancer cells. In addition, coupling PD-L1 to NPs maintains the affinity of the drug loaded NPs. Confocal microscopy was performed to observe the phagocytosis of FITC-labeled SP/Ls and PD-SP/Ls particles by liver cancer cell lines (Figure 4 (a)). The results showed that the phagocytosis efficiency of PD-SP/Ls particles by HepG2 cells was significantly higher than in the SP/Ls group, consistent with the results in Figure 3. Of course, the PD-SP/Ls demonstrated higher FITC fluorescence positive ratio (90.6%) in the HepG2 cells compared with the SP/Ls (90.6%). In contrast, the free FITC group exhibited
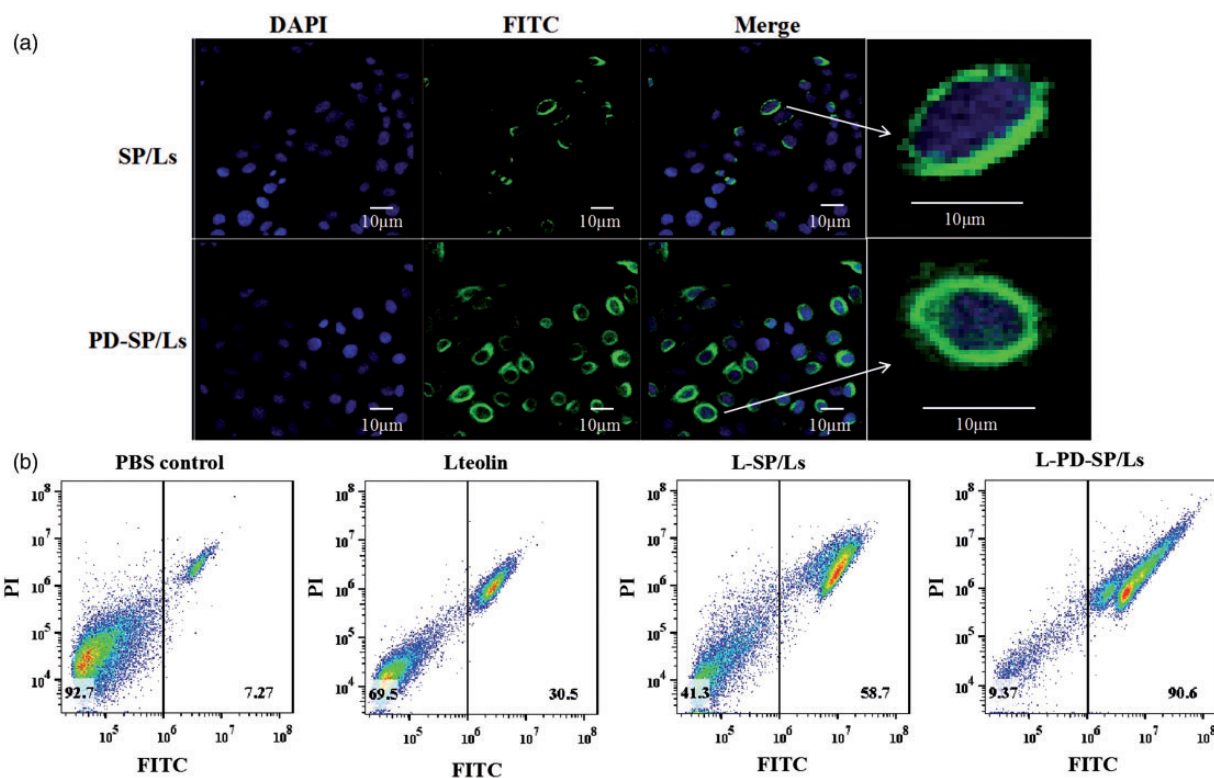

Figure 3. (a) Results of MTT assay after 6, 12, 24 and 48 hours of incubation. (b) Cytotoxicity of different luteolin loaded NPs, measured by MTT assay after incubation for 24 hours with different concentrations.

Figure 4. (a) Images of cellular uptake by confocal laser scanning microscopy. (b) Flow cytometry analysis of different luteolin loaded NPs.

more little FITC uptake efficiency (30.5%) at the same condition (Figure 4(b)). Under the same drug concentration, the targeting effects of PD-SP/Ls could improve the accumulation of luteolin in tumor cells, thereby enhancing the inhibition of cells by drugs.

Detection of cell migration

Tumor cells still have migration ability in vitro. Using the experimental model of cell-induced wound healing in vitro, cell scratch method was used to determine the movement migration ability of HepG2 cells under the action of L-SP/Ls and L-PD-SP/Ls. The results of the wound healing test, as shown in Figure 5, demonstrated that the average distance of migration of luteolin-loaded non-targeted SP/Ls was $155.0 \pm 17.1 \, \mu m$, as compared with $64.0 \pm 4.9 \, \mu m$ in the PD-SP/Ls group, and the difference was significant. After treatment with 18 hours, the cell state of L-PD-SP/Ls group was not good with obviously the number decreases and the cell atrophy. This indicated that the PD-SP/Ls constructed displayed excellent targeting ability and could significantly inhibit the migration of HepG2 cells.
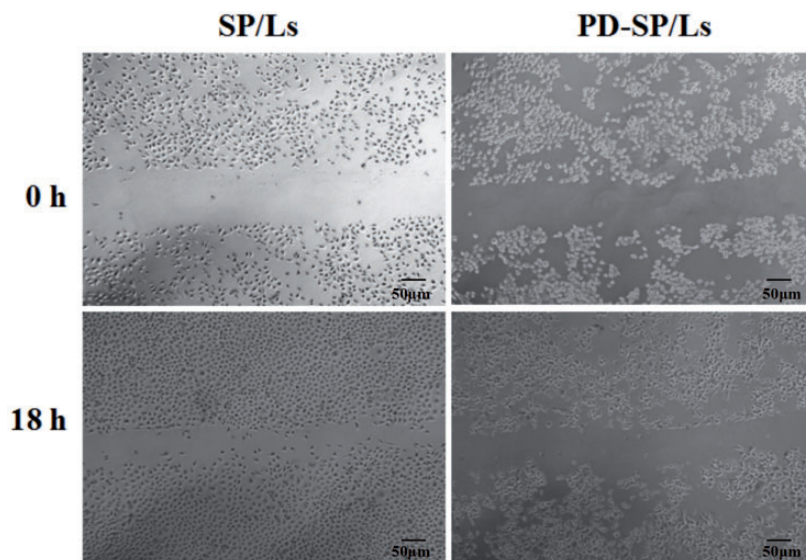
Detection of expression of bcl-2 mRNA using RT-PCR

Apoptosis may occur through endogenous mitochondrial dysfunction pathways. Mitochondrial apoptotic pathway up-regulates Bcl-2 family proteins, which are anti-apoptotic proteins, inhibits mPTP, and blocks the release of cytochrome C. The expression of Bcl-2 mRNA was detected to verify the factors leading to cell apoptosis. Western blot results showed that Bcl-2 protein expression was decreased in the microsphere group compared with the control group. The L-PD-SP/Ls group had the lowest expression level (Figure 6(a)). Of course, compared with the cell control group (CON), the expression of Bcl-2 mRNA in the luteolin-loaded NPs was significantly decreased after 72 hours, and the decrease of Bcl-2 mRNA was more significant in the PD-SP/Ls group than in the SP/Ls group, with statistically significant differences ($p < 0.05$) (Figure 6(b)). The above results indicated that the apoptosis induced by luteolin was mediated by mitochondrial apoptosis pathway, and the targeted delivery of PD-L1 could significantly inhibit cell survival and promote apoptosis.
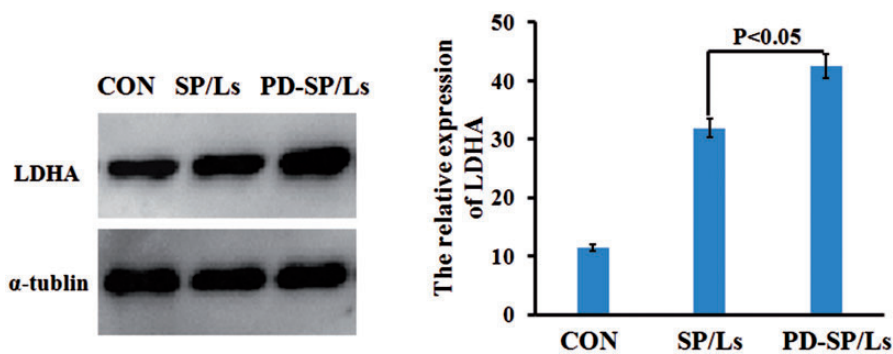
Detection of LDH release in HepG2 cells

Figure 7 showed that the LDH release in cells of the control group was low ($11.4 \pm 3.6 \, U.L^{-1}$) and significantly increased after the intervention of luteolin drug. LDH levels in PD-L1 targeted group and non-targeted group reached $42.5 \pm 2.6 \, U.L^{-1}$ and $31.9 \pm 3.2 \, U.L^{-1}$, respectively, with statistically significant differences

Figure 5. The results of wound healing assay for SP/Ls and PD-SP/Ls.
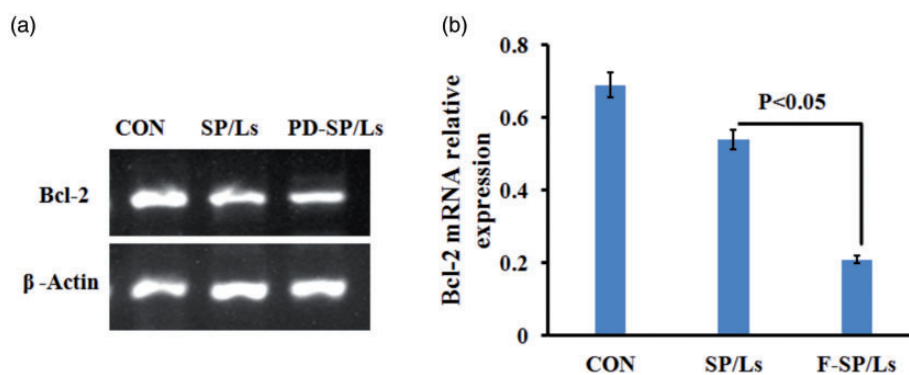
Figure 6. (a) Detection of Bcl-2 protein expressions in HepG2 cells using Western blot. (b) Detection of Bcl-2 mRNA expression in HepG2 cells by Q-PCR.

Figure 7. Detection of LDH protein expressions in HepG2 cells using Western blot.

between the two controls ($p < 0.05$). The results of western blot method were consistent with those of LDH test kit. The above data indicated that luteolin significantly inhibited the survival of HepG2 cells and increased LDH release, indicating that luteolin had significant hepatocellular toxicity, while the targeting function of PD-L1 hepatocellular carcinoma cells effectively increased the uptake ability of hepatocellular

carcinoma cells and increased the inhibition ability of drugs to hepatocellular carcinoma cells.

Conclusions

In this study, we successfully constructed the luteolin-loaded nano-liposome targeting PD-1 receptor on the surface of liver cancer. It could be used for the targeted delivery to liver cancer cells, which significantly increased the sensitivity of liver cancer cells to luteolin and reduced the concentration of drugs used while achieving satisfactory effects of tumor inhibition. In this study, we found that luteolin could be used to increase the expression of LDH, thereby limiting tumor growth by interfering with the mitochondrial pathway of tumor cells. Besides, the PD-L1 targeting-modified nano-drug delivery system could potentiate drug function effectively, as compared with non-targeted systems, whereas the mechanisms underlying it still merit further studies.

Declaration of conflicting interests

Funding

ORCID iD

Bing Wang (iD) https://orcid.org/0000-0002-2089-8888

References

1. Ralhan R and Kaur J. Alkylating agents and cancer therapy. *Expert Opin Ther Patents* 2007; 17: 1061–1075.
2. Maemondo M, Inoue A, Kobayashi K, Sugawara, et al. Gefitinib or chemotherapy for non–small-cell lung cancer with mutated EGFR. *N Engl J Med* 2010; 362: 2380–2388.
3. Singh A and Settleman J. Emt, cancer stem cells and drug resistance: an emerging axis of evil in the war on cancer. *Oncogene* 2010; 29: 4741–4751.
4. De VS, Suleiman AHM, Schellens AA, et al. Pharmacodynamic modeling of adverse effects of anti-cancer drug treatment. *Eur J Clin Pharmacol* 2016; 72: 645–653.
5. Niwa K, Hashimoto M and Tamaya T. Effects of juzen-taiho-to and M-CSF on thrombocytopenia induced by anti-cancer drugs in gynecologic malignances. *Kampo Med Nihon Toyo Igaku Zasshi* 2000; 51: 447–454.
6. Yoo DR, Jang YH, Jeon YK, et al. Proteomic identification of anti-cancer proteins in luteolin-treated human hepatoma huh-7 cells. *Cancer Letters* 2009; 282: 48–54.
7. Hwang J T and Yang HJ. Anti-cancer effects of luteolin and its novel mechanism in HepG2 hepatocarcinoma cell. *KSBB J* 2010; 25: 507–512.
8. Lipka D, Filipczak N, Kozubek A, et al. Folate targeted vitamin c based liposomal formulation of epirubicin – novel nano drug delivery system, which ensures fast drug release. In *IIX Multidyscyplinarna Konferencja Nauki o Leku*, Wrocław, Poland, May 2014. http://science24.com/paper/31195
9. Dong Y, Cao R, Li Y, et al. Folate-conjugated nano-diamond for tumor-targeted drug delivery. *RSC Adv* 2015; 5: 82711–82716.
10. Downer J, Sevinsky JR, Ahn NG, et al. Incorporating expression data in metabolic modeling: a case study of lactate dehydrogenase. *J Theor Biol* 2006; 240: 464–474.
11. Gaspar P, Al-Bayati FAY, Andrew PW, et al. Lactate dehydrogenase is the key enzyme for pneumococcal pyruvate metabolism and pneumococcal survival in blood. *Infect Immun* 2014; 82: 5099–5109.
12. Georgiev P, Holmes RS and Masters CJ. Extracellular lactate dehydrogenase hormonal influences on the oviducal isoenzymes. *BBA—Gen Sub* 1970; 222: 155–162.
13. Piasentin N, Milotti E and Chignola R. The control of acidity in tumor cells: a biophysical model. *Sci Rep* 2020; 10: 13613.
14. Onyango JO. *Improving the pH-response of pHLIP insertion at tumor acidity for targeted drug delivery against cancer: biophysical studies in model membranes and evaluations in cells.* Dissertations and Theses—Gradworks, State University of New York at Binghamton, USA, 2014.
15. Xin L, Cao JQ, Liu C, et al. Evaluation of rMETase-Loaded stealth PLGA/liposomes modified with anti-CAGE scFV for treatment of gastric carcinoma. *J Biomed Nanotechnol* 2015; 11: 1153–1161.
16. Yiyin C, Le VM, Jiawen L, et al. Baicalin loaded in folate-PEG modified liposomes for enhanced stability and tumor targeting. *Colloids Surf B Biointerf* 2016; 140: 74–82.
17. Zhang C, Chen Z, Zhou X, et al. Cantharidin induces G2/M phase arrest and apoptosis in human gastric cancer SGC-7901 and BGC-823 cells. *Oncol Lett* 2014; 8: 2721–2726.
18. Chen XQ, Wang SJ, Du JZ, et al. Diversities in hepatic HIF-1, IGF-I/IGFBP-1, LDH/ICD, and their mRNA expressions induced by CoCl2 in Qinghai-Tibetan Plateau mammals and sea level mice. *Am J Physiol Regulat Integr Comparat Physiol* 2007; 292: R516–R526.
19. Jouaville LF, Fellmann N, Coudert J, et al. Skeletal muscle expression of LDH and monocarboxylate transporters in growing rats submitted to protein malnutrition. *Eur J Nutr* 2006; 45: 355–362.
20. Tan C, Xue J, Abbas S, et al. Liposome as a delivery system for carotenoids: comparative antioxidant activity of carotenoids as measured by ferric reducing antioxidant power, DPPH assay and lipid peroxidation. *J Agric Food Chem* 2014; 62: 6726–6735.
21. Tan C, Zhang Y, Abbas S, et al. Modulation of the carotenoid bioaccessibility through liposomal encapsulation. *Colloids Surf B Biointerf* 2014; 123: 692–700.